Original Article

# Potential Clinical Risk of Inflammation and Toxicity from Rare-Earth Nanoparticles in Mice

**Jian-Ping Chen[1], Song-Sheng Shi[2], Gui-Fen Liu[3], Yan Chen[1], Shui-Shun Zheng[4], Xiao-Bin Wang[1], Ru-Hui Lin[5], Hong-Xing He[6], Cai-Hou Lin[1]**

[1]Department of Neurosurgery, Fujian Medical University Union Hospital, Fuzhou, Fujian 350001, China
[2]Institute of Neurosurgery, Fujian Province, Fuzhou, Fujian 35001, China
[3]Department of Obstetrics and Gynecologic Oncology, Fujian Provincial Maternity and Children's Hospital, Affiliated Hospital of Fujian Medical University, Fuzhou, Fujian 350001, China
[4]Department of Neurosurgery, Zhangzhou Municipal Hospital Affiliated to Fujian Medical University, Zhangzhou, Fujian 363000, China
[5]Department of Biomedical Research, Academy of Integrative Medicine, Fujian University of Traditional Chinese Medicine, Fuzhou, Fujian 350108, China
[6]Laboratory Animal Center, Fujian Medical University, Fuzhou, Fujian 350108, China

Jian-Ping Chen and Song-Sheng Shi contributed equally to this work.

## Abstract

**Background:** Nanotechnology is emerging as a promising tool to perform noninvasive therapy and optical imaging. However, nanomedicine may pose a potential risk of toxicity during *in vivo* applications. In this study, we aimed to investigate the potential toxicity of rare-earth nanoparticles (RENPs) using mice as models.

**Methods:** We synthesized RENPs through a typical co-precipitation method. Institute of Cancer Research (ICR) mice were randomly divided into seven groups including a control group and six experimental groups (10 mice per group). ICR mice were intravenously injected with bare RENPs at a daily dose of 0, 0.5, 1.0, and 1.5 mg/kg for 7 days. To evaluate the toxicity of these nanoparticles in mice, magnetic resonance imaging (MRI) was performed to assess their uptake in mice. In addition, hematological and biochemical analyses were conducted to evaluate any impairment in the organ functions of ICR mice. The analysis of variance (ANOVA) followed by a one-way ANOVA test was used in this study. A repeated measures' analysis was used to determine any significant differences in white blood cell (WBC), alanine aminotransferase (ALT), and creatinine (CREA) levels at different evaluation times in each group.

**Results:** We demonstrated the successful synthesis of two different sizes (10 nm and 100 nm) of RENPs. Their physical properties were characterized by transmission electron microscopy and a 980 nm laser diode. Results of MRI study revealed the distribution and circulation of the RENPs in the liver. In addition, the hematological analysis found an increase of WBCs to $(8.69 \pm 0.85) \times 10^9$/L at the 28$^{th}$ day, which is indicative of inflammation in the mouse treated with 1.5 mg/kg $NaYbF_4$:Er nanoparticles. Furthermore, the biochemical analysis indicated increased levels of ALT ([64.20 ± 15.50] U/L) and CREA ([27.80 ± 3.56] μmol/L) at the 28$^{th}$ day, particularly those injected with 1.5 mg/kg $NaYbF_4$:Er nanoparticles. These results suggested the physiological and pathological damage caused by these nanoparticles to the organs and tissues of mice, especially to liver and kidney.

**Conclusion:** The use of bare RENPs may cause possible hepatotoxicity and nephritictoxicity in mice.

**Key words:** Bioanalysis; Hemanalysis; Hepatotoxicity; Nephritictoxicity; Rare-Earth Nanoparticle

## Introduction

Nanotechnology is emerging as a promising tool to restore, maintain, or enhance tissue and organ functions.[1-3] Nanoparticles have been widely applied to produce material structures that mimic biological functions or serve as drug delivery vehicles.[4,5] For instance, the rare-earth-doped nanoparticles are attractive candidates in nanomedicine,

Access this article online

Quick Response Code:

Website: www.cmj.org

DOI: 10.4103/0366-6999.235105

**Address for correspondence:** Dr. Cai-Hou Lin, Department of Neurosurgery, Fujian Medical University Union Hospital, Fuzhou, Fujian 350001, China
E-Mail: lincai76@163.com



**Received:** 01-04-2018 **Edited by:** Yuan-Yuan Ji
**How to cite this article:** Chen JP, Shi SS, Liu GF, Chen Y, Zheng SS, Wang XB, Lin RH, He HX, Lin CH. Potential Clinical Risk of Inflammation and Toxicity from Rare-Earth Nanoparticles in Mice. Chin Med J 2018;131:1591-7.

owing to their applications as near-infrared nanoprobes to control cell growth or biomaterial degradation.[6-8] For safety and efficiency of these particles, much attention has been paid to the toxicological evaluation of rare-earth nanomedicine in biological systems.[9] In previous studies, various toxicity assays were conducted using the nanoparticles coated with peptides, ligands, or other chemical compounds.[10-14] Surface coating may influence the dimensions, morphologies, and properties of the nanoparticles and lead to potential misunderstanding with respect to their toxicity in response to the ionic leakage in the body.[15] Therefore, the applications of these nanoparticles in nanomedicine demand a systemic investigation of their cellular toxicity *in vivo*.

Rare-earth-doped nanoparticles without surface protection were recently shown to exhibit potential cytotoxicity, owing to their ability to induce ATP quenching upon binding to the phosphate group of intracellular ATP.[16] In addition, Maria *et al*.[17] found that bare rare-earth nanoparticles (RENPs) are toxic to hippocampal cells *in vitro*. So far, most reported studies have focused on the *in vitro* toxicity assays; however, the fate of RENPs circulating in the blood vessels and tissues *in vivo* is much more complicated. Therefore, *in vivo* studies are desirable to accurately assess the toxicity of these nanoparticles.

In this study, we present a systemic investigation for *in vivo* evaluation of hepatotoxicity, nephrotoxicity, and fate in blood circulation of bare RENPs in mice. Two different RENPs were intravenously injected into the mice, and their toxicity was studied by the combination of biochemical analysis and magnetic resonance imaging (MRI) [Figure 1a]. We demonstrated that the RENPs cause obvious inflammation-related effects in the mouse, possibly related to ATP quenching effects such that the ATP molecules lose their functions by the strong binding interaction between the phosphate group and rare-earth ions [Figure 1b]. Our study on the intrinsic toxicity of these nanoparticles may offer a valuable theoretical basis for evaluation of the toxicity of rare-earth nanomaterials used regenerative medicine.

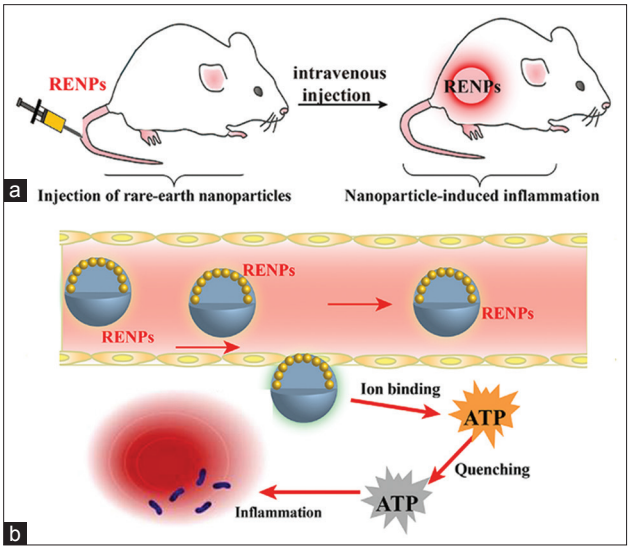


**Figure 1:** (a) A schematic representation of RENPs intravenously injected in the mouse. (b) The injected rare-earth nanoparticles may induce ATP quenching and inflammation in the mouse. ATP quenching was caused by the strong binding interaction between its phosphate group and rare-earth ions. RENPs: Rare-earth nanoparticles.

## Methods

### Chemicals

The compounds 1-octadecene (90%), oleic acid (90%), $Y(CH_3CO_2)_3{\cdot}xH_2O$ (99.9%), $Gd(CH_3CO_2)_3{\cdot}xH_2O$ (99.9%), $Er(CH_3CO_2)_3{\cdot}xH_2O$ (99.9%), $Yb(CH_3CO_2)_3{\cdot}4H_2O$ (99.9%), ammonium fluoride ($NH_4F$, 99%), and sodium hydroxide (NaOH, 98%) were purchased from Sigma-Aldrich, Shanghai, China. Isoflurane anesthesia was purchased from Baxter, USA.

### Synthesis of rare-earth nanoparticles

RENPs of $NaGdF_4$:Yb/Er (18/2%) and $NaYbF_4$:Er (2%) were synthesized with a co-precipitation method, with some modifications in our previously reported protocol.[18] In brief, an aqueous solution (2 ml) of 0.2 mol/L Gd $(CH_3CO_2)_3$, 0.2 mol/L Er $(CH_3CO_2)_3$, and 0.2 mol/L Yb $(CH_3CO_2)_3$ was prepared in a 50 ml two-neck flask. Oleic acid (3 ml) and octadecene (7 ml) were injected into the flask, and the resulting mixture was heated at 150°C for 2 h under an oil bath condition. The precursor was cooled to 50°C and moved to the heating mantle with a temperature controller. A fresh mixture of 2 ml NaOH (0.5 mol/L in methanol) and 4 ml $NH_4F$ (0.4 mol/L in methanol) was added, and the resultant mixture was stirred for 2 h, a step that is essential to prepare uniform RENPs. The solution was heated to 100°C and degassed with argon for 30 min to remove the methanol and oxygen. The resultant solution was finally heated to 290°C for 2 h. The product was cooled to room temperature, and the synthesized nanoparticles were precipitated out with ethanol. The nanoparticles were collected by 1680 ×*g* centrifugation for 10 min, rewashed with ethanol, and finally dispersed in 4 ml of cyclohexane. The preparation of bare RENPs was conducted with a ligand-free method as previously reported.[18]

### Physical characterization of rare-earth nanoparticles

Luminescence spectra of the RENPs were measured following excitation with a 980 nm diode laser (FC-980, Changchun Optics, China) using a phosphorescence spectrometer (FSP920, Edinburgh, UK). Transmission electron microscopy (TEM) measurements were performed on a 200 kV JEM-2100F transmission electron microscope (JEOL, Japan). Nanoparticle hydrodynamic size and zeta potential were measured using dynamic light scattering (DLS) on a Zetasizer Nanoparticle analyzer series (Malvern Instruments Ltd., England).

### Intravenous injection of rare-earth nanoparticles in mice

The animal study was approved by the Institutional Animal Care and Use Committee of the University. Every effort was made to reduce the suffering of animals and minimize their number. All procedures involved in this study

were in accordance with our institutional guidelines that complied with the international ethics for animal use. In our experiment, adult male Institute of Cancer Research (ICR) mice (weight, 20–25 g; age: 6–8 weeks) were purchased from the Laboratory Animal Center of Fujian Medical University (Batch number: SCXK (Viet) 2012-0001). Mice were maintained in a 12 h light/dark environment and provided with food and water. The mice were acclimatized for 1 week before the experiment. RENPs ($NaGdF_4$:Yb/Er or $NaYbF_4$:Er-based nanoparticles) were intravenously injected at doses of 0, 0.5, 1.0, and 1.5 mg/kg body weight. The mice were weighed daily before receiving an intravenous injection. The symptoms were observed and recorded carefully for 28 days.

### Blood biochemical assay

The blood samples obtained from ICR mice were used for biochemical analysis. To minimize pain in the experimental animals, mice were given a general anesthetic using 20% urethane, and the blood was withdrawn through the abdominal artery after 7, 14, and 28 days. The serum was obtained by the centrifugation of whole blood at 3000 r/min for 15 min and analyzed using the automatic blood analyzer. During the experiments, all animals received humane care according to the criteria outlined in the "Guide for the Care and Use of Laboratory Animals" prepared by China Government.

### Magnetic resonance imaging characterization

*In vivo* MRI of mice livers was conducted using a 7 T, 20 cm bore magnet (70/20 USR Bruker, Germany) after intravenous administration of nanoparticles every morning for 7 days. Mice were maintained under isoflurane anesthesia (1.2% ± 0.5%) throughout imaging and were placed in a prone position on an animal bed and then slide in the center of a magnet bore. The parameters were as follows: $T_2$ mapping was acquired using MSME_$T_2$ (Multi-Slice Multi Echo) sequence (repetition time [TR] = 0.5 s, effective echo time [TE] = 17.0 ms, field of view = 30.00 × 30.00 mm). Images were reconstructed at 100 μm isotropic resolution, while the acquisition time was ~1 h.

### Statistical analysis

Experiments were repeated at least thrice ($n \geq 3$), and each group in the behavior studies had at least ten mice. Data are expressed as mean ± standard deviation (SD) and analyzed with the analysis of variance (ANOVA) followed by a one-way ANOVA test. A repeated measures' analysis was used to determine any significant differences in white blood cell (WBC), alanine aminotransferase (ALT), and creatinine (CREA) levels at different evaluation times in each group. Statistical analysis was performed with SPSS 19.0 software (SPSS Inc., Chicago, IL, USA). Significance was set at $P \leq 0.05$.

## Results

### Characterization of rare-earth nanoparticles

To examine the effects of particle size on toxicity in mice, two different sizes of RENPs were synthesized. In a typical experiment, the size of the RENPs was adjusted by controlling $Yb^{3+}$ dopant concentration in the host. The resulting RENPs were characterized with TEM. As shown in Figure 2a and 2b, the size of the $NaGdF_4$:Yb/Er and

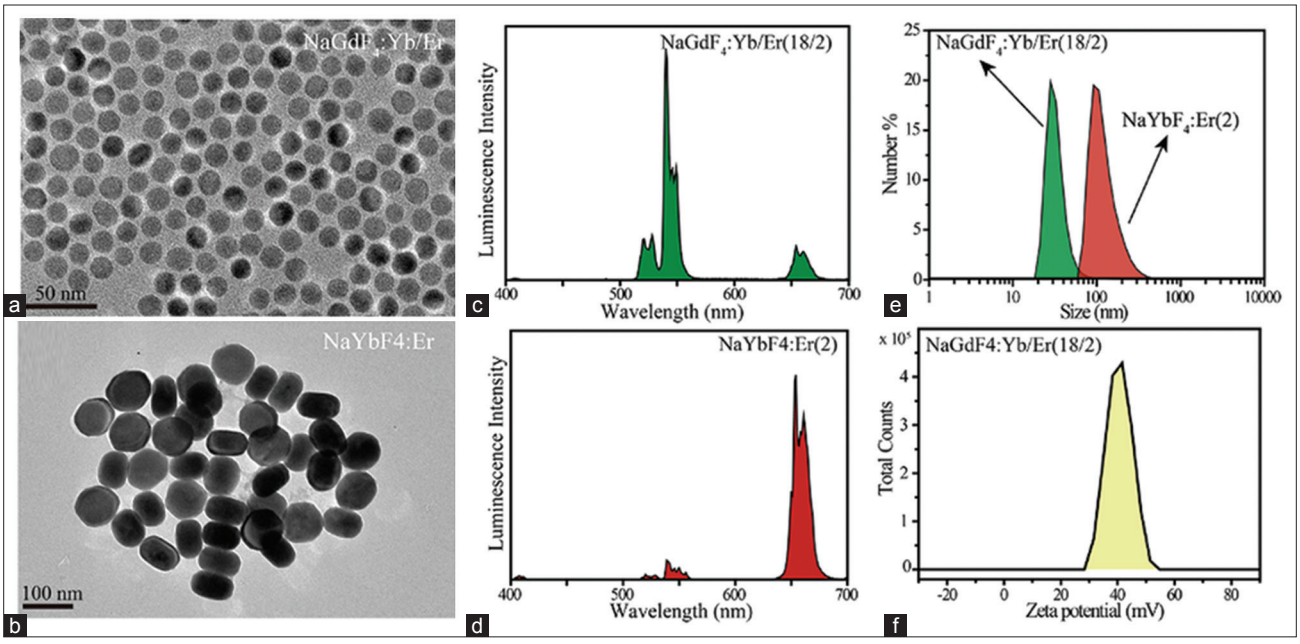


**Figure 2:** (a and b) Low-resolution TEM image of the synthesized nanoparticles with different rare-earth dopants. NaGdF4:Yb/Er (18/2) and NaYbF4:Er (2% mol). (c and d) Luminescence emission spectra of nanoparticles with different rare-earth dopants in cyclohexane. NaGdF4:Yb/Er (18/2) and NaYbF4:Er (2% mol). The spectra were recorded after excitation with a 980 nm laser. (e) Dynamic light scattering measurement of the rare-earth nanoparticles dispersed in cell culture media. (f) Zeta potential of NaGdF4:Yb/Er (18/2) nanoparticles dispersed in water. TEM: Transmission electron microscopy.

$NaYbF_4$:Er RENPs was 10 nm and 100 nm, respectively. Furthermore, fluorescence spectra were measured at an excitation of 980 nm diode laser [Figure 2c and 2d]. These results demonstrated the successful preparation of the desired RENPs. For their application in mice, the synthesized hydrophobic nanoparticles were made hydrophilic with ligand-free method. In addition, we measured the zeta potential and hydrodynamic size in a dispersion medium to study the dispersion of these particles in solution. As shown in Figure 2e, the prepared nanoparticles are well dispersed in cell culture media after a ligand-free treatment. The measurement of zeta potential further showed that the bare rare-earth-doped nanoparticles had positive charges on their surfaces [Figure 2f], suggestive of their ability to interact with the phosphate group of intracellular ATP.

## *In vivo* magnetic resonance imaging for nanoparticle uptake evaluation

To study the uptake of RENPs, mice were intravenously injected with bare RENPs on every morning for 7 days. To observe the nanoparticle circulation in the mice, MRI was carried out to study the RENPs present in the mouse liver. As shown in Figure 3, distinct T2 hyperintense signals were detected in the mouse liver. Our results showed that the MRI signals in mice liver were enhanced after 1 h of injection, and the signal intensity disappeared after 3 h. This result suggests that the RENPs may be uptaken in the liver, followed by their clearance from the liver. The dynamic observation of the RENPs may help us better understand the metabolism pathway of the nanoparticles in the animal body.

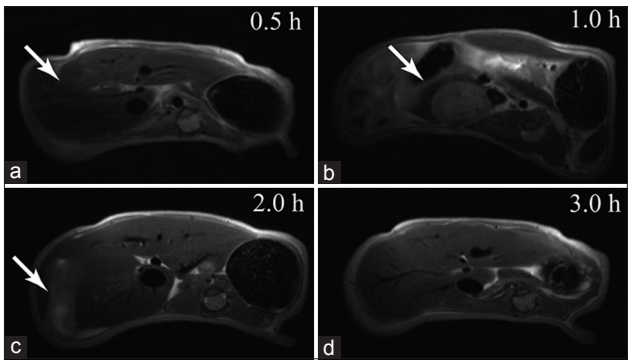


**Figure 3:** T2-weighted images of mice liver as a function of time after rare-earth nanoparticle injection. The MRI images (a-d) were recorded after 0.5, 1, 2, and 3 h, respectively. The white arrows indicated the evidence of the rare-earth nanoparticles uptaken in the liver of the mouse. MRI: Magnetic resonance imaging.

## Hematological analysis for toxicological evaluation

To investigate the effect of RENPs on the mouse, hematological analysis was performed after 7, 14, and 28 days from the injection of bare RENPs. As shown in Figure 4a, 4b and Table 1, mice injected with $NaYbF_4$:Er and $NaGdF_4$:Yb/Er nanoparticles showed an increased level of WBCs as compared with control mice. Mice injected with a high dose of 1.5 mg/kg $NaGdF_4$:Yb/Er nanoparticles (or $NaYbF_4$:Er nanoparticles) showed an obvious abnormal change in the level of WBC as compared to those injected with 0.5 and 1.0 mg/kg $NaGdF_4$:Yb/Er nanoparticles (or $NaYbF_4$:Er nanoparticles). In addition, the level of WBCs in $NaYbF_4$:Er treatment group increased as compared to that in $NaGdF_4$:Yb/Er treatment group. WBCs, also called as leukocytes, originate in the bone marrow but circulate throughout the bloodstream. Any abnormal change in WBCs levels is suggestive of the occurrence of inflammation following the invasion of the RENPs. This observation may be associated with the presence of rare-earth ions on the surface of bare nanoparticles or ion leakage that resulted in their strong binding to ATP molecules in cells. As a consequence, ATP quenching was observed that resulted in cell apoptosis and autophagy. The clearance of the damaged cells may be likely responsible for the inflammation observed in these mice. Furthermore, the injection of large-sized NaYbF4:Er nanoparticles resulted in higher levels of WBCs as compared to small-sized NaGdF4:Yb/Er nanoparticles under same experimental condition. We suggest that the large RENPs may not be efficiently cleared from the blood system. Further analysis of the red blood cell and platelet levels revealed the absence of any obvious damage caused to the blood function by RENPs.

## Biochemical analysis for toxicological evaluation

We examined the influence of RENPs on the liver and kidney in mice. Biochemical analysis was carried out to evaluate the toxicity associated with bare RENPs after their injection in mice. In particular, CREA is a waste product indicative

**Table 1: Hematological analysis in mice treated with rare-earth nanoparticles* ($n$ = 10)**

| Parameters | Time points | Control | $NaGdF_4$:Yb/Er-0.5 | $NaGdF_4$:Yb/Er-1.0 | $NaGdF_4$:Yb/Er-1.5 | $NaYdF_4$:Er-0.5 | $NaYdF_4$:Er-1.0 | $NaYdF_4$:Er-1.5 |
|---|---|---|---|---|---|---|---|---|
| WBC ($\times10^9$/L) | 7th | 3.02 ± 0.33 | 4.05 ± 0.29 | 4.65 ± 0.24 | 5.52 ± 0.38 | 6.26 ± 0.22 | 7.16 ± 0.46 | 8.81 ± 0.69 |
| | 14th | 3.31 ± 0.19 | 4.19 ± 0.14 | 4.56 ± 0.12 | 5.28 ± 0.29 | 5.75 ± 0.22 | 6.55 ± 0.40 | 7.92 ± 0.83 |
| | 28th | 2.44 ± 1.09 | 4.05 ± 0.29 | 4.89 ± 0.52 | 6.32 ± 1.57 | 5.79 ± 0.43 | 6.72 ± 0.35 | 8.69 ± 0.85 |
| RBC ($\times10^{12}$/L) | 7th | 9.87 ± 0.85 | 9.31 ± 1.04 | 10.41 ± 0.52 | 10.10 ± 0.76 | 9.84 ± 0.90 | 9.90 ± 0.79 | 10.16 ± 0.71 |
| | 14th | 10.16 ± 0.80 | 9.91 ± 0.75 | 9.24 ± 1.90 | 9.97 ± 0.64 | 9.91 ± 0.87 | 9.77 ± 0.22 | 10.75 ± 0.20 |
| | 28th | 9.63 ± 0.70 | 9.31 ± 1.04 | 10.42 ± 0.52 | 9.98 ± 1.23 | 10.32 ± 0.49 | 9.76 ± 0.67 | 9.92 ± 0.42 |
| PLT ($\times10^{11}$/L) | 7th | 15.60 ± 3.74 | 15.88 ± 1.30 | 14.65 ± 1.96 | 14.36 ± 3.13 | 16.84 ± 3.78 | 15.77 ± 2.03 | 12.89 ± 3.53 |
| | 14th | 14.79 ± 2.29 | 15.67 ± 2.05 | 13.83 ± 2.56 | 14.35 ± 1.75 | 14.92 ± 2.50 | 15.37 ± 1.63 | 14.58 ± 2.56 |
| | 28th | 12.43 ± 7.06 | 15.88 ± 1.30 | 14.78 ± 1.81 | 16.88 ± 2.60 | 15.88 ± 3.90 | 14.23 ± 2.73 | 12.73 ± 3.21 |

*The data was acquired on day 7, 14, and 28 after injection with rare-earth nanoparticles. RBC: Red blood cell; PLT: Platelet; WBC: White blood cell.

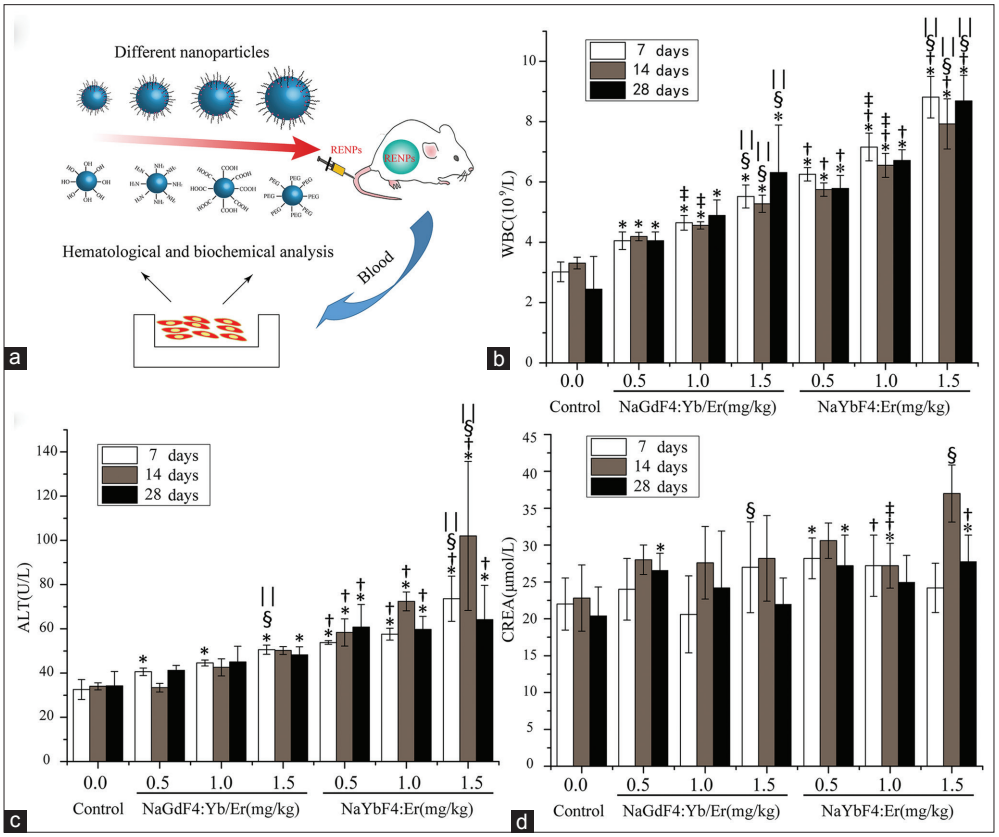


**Figure 4:** (a) ICR mice were subcutaneously injected with different bare rare-earth nanoparticles. Hematological and biochemical analyses were performed to evaluate any impairment in organ functions. (b-d) Effects of rare-earth nanoparticles on WBC, ALT, and CREA levels in ICR mice. The data were acquired on day 7, 14, and 28. *Comparison between control and groups injected with the same type of nanoparticles at different doses ($P < 0.05$). †Comparison between groups injected with different nanoparticles at the same dose ($P < 0.05$). ‡Comparison between two groups treated with 0.5 and 1.0 mg/kg rare-earth nanoparticle of the same type ($P < 0.05$). §Comparison between two groups treated with 1.5 and 1.0 mg/kg rare-earth nanoparticle of the same type ($P < 0.05$). ‖Comparison between two groups treated with 1.5 and 0.5 mg/kg of rare-earth nanoparticle of the same type ($P < 0.05$). ICR: Institute of Cancer Research; WBC: White blood cell; ALT: Alanine aminotransferase; CREA: Creatinine.

of the kidney function and high level of CREA in the blood may reveal the malfunctioning or failure of kidneys. In comparison with the control mice, those injected with a high dose (1.5 mg/kg) of NaGdF4:Yb/Er nanoparticles showed an abnormal change in the level of CREA on day 28 after injection [Figure 4c and Table 2]. These results suggest that the RENPs only caused minor nephritic toxicity but caused obvious hepatotoxicity in mice, as evaluated by ALT level in mice blood. ALT is an enzyme produced in the liver cells; an increase in serum ALT level is indicative of the damage or inflammation of the liver. As shown in Figure 4d and Table 2, mice injected with RENPs (experimental groups) had an obvious increase in ALT levels as compared with the control mice. In comparison with the small-sized NaGdF4:Yb/Er nanoparticles, large-sized NaYbF4:Er nanoparticles caused an obvious increase in ALT levels. This observation could be explained by the enrichment of large-sized nanoparticles in the mice liver that may have caused severe damage to the liver. At day 14, the increase in the total bilirubin level was more prominent, suggestive of an increase in the metabolic disturbance in mouse liver. This result indicates the enhanced clearance of RENPs from the mouse liver by day 14. No obvious variations in the level of aspartate aminotransferase, total proteins, and uric acid were observed. Taken together, bare RENPs exhibited nonnegligible risk upon their direct application in the animal body.

## Discussion

In this study, we have performed *in vivo* evaluation of hepatotoxicity and nephritic toxicity caused by two different sizes of RENPs in mice. In previous studies, RENPs' surface coated with biomolecules, polymers, or silica layers exhibited low cytotoxicity in mice.[19,20] As the coating material may influence the accurate assessment of the potential toxicity of bare nanoparticles or ionic leakage in mice, the intrinsic cytotoxicity of bare nanoparticles was studied. In this study, we used a hydrophilic ligand-free method to prepare bare RENPs that allowed the study of the intrinsic toxicity of RENPs in the animal body. TEM characterization and fluorescence spectrum measurement revealed the successful synthesis of RENPs. Although it was reported that ligand-free RENPs can induce a decrease in cell viability, possibly associated with the deprivation of intracellular ATP in live cells, few studies are reported to examine the toxic effects of bare RENPs *in vivo*.

**Table 2: Effects of rare-earth nanoparticles on biochemical analysis* ($n$ = 10)**

| Parameters | Time points | Control | $NaGdF_4$:Yb/Er-0.5 | $NaGdF_4$:Yb/Er-1.0 | $NaGdF_4$:Yb/Er-1.5 | $NaYdF_4$:Er-0.5 | $NaYdF_4$:Er-1.0 | $NaYdF_4$:Er-1.5 |
|---|---|---|---|---|---|---|---|---|
| TBIL (μmol/L) | 7th | 3.96 ± 0.77 | 4.00 ± 0.81 | 3.92 ± 0.88 | 3.78 ± 0.63 | 4.62 ± 1.00 | 4.40 ± 0.55 | 4.18 ± 0.33 |
| | 14th | 4.02 ± 0.94 | 21.42 ± 5.98 | 18.58 ± 3.81 | 16.98 ± 2.98 | 17.14 ± 6.17 | 19.50 ± 8.17 | 15.88 ± 5.25 |
| | 28th | 3.86 ± 0.82 | 4.36 ± 0.67 | 3.76 ± 0.55 | 3.94 ± 0.88 | 4.72 ± 0.54 | 3.94 ± 0.42 | 4.28 ± 0.98 |
| ALT (U/L) | 7th | 32.60 ± 4.51 | 40.60 ± 1.67 | 44.60 ± 1.34 | 50.60 ± 2.07 | 53.80 ± 0.84 | 57.60 ± 2.70 | 73.60 ± 10.21 |
| | 14th | 34.00 ± 1.58 | 33.40 ± 1.95 | 42.60 ± 3.85 | 50.20 ± 1.79 | 58.40 ± 6.15 | 72.40 ± 4.22 | 102.00 ± 33.70 |
| | 28th | 34.20 ± 6.53 | 41.20 ± 2.28 | 45.00 ± 7.10 | 48.20 ± 3.70 | 60.80 ± 10.26 | 59.80 ± 5.85 | 64.20 ± 15.50 |
| AST (U/L) | 7th | 124.60 ± 13.40 | 141.00 ± 35.92 | 122.80 ± 14.84 | 145.60 ± 29.36 | 154.80 ± 43.27 | 142.60 ± 18.20 | 187.80 ± 58.34 |
| | 14th | 119.60 ± 16.74 | 131.20 ± 13.08 | 136.00 ± 19.69 | 145.60 ± 15.77 | 142.80 ± 30.64 | 157.80 ± 24.40 | 197.00 ± 40.04 |
| | 28th | 116.40 ± 10.09 | 136.20 ± 38.13 | 136.80 ± 5.93 | 133.60 ± 29.59 | 153.60 ± 16.26 | 167.40 ± 52.35 | 175.20 ± 55.11 |
| TP (g/L) | 7th | 54.48 ± 0.97 | 55.76 ± 2.08 | 54.52 ± 4.72 | 51.64 ± 3.93 | 55.04 ± 4.73 | 56.60 ± 1.54 | 57.12 ± 4.99 |
| | 14th | 54.00 ± 3.01 | 52.08 ± 2.28 | 52.56 ± 1.97 | 57.84 ± 4.37 | 45.56 ± 17.14 | 16.02 ± 1.34 | 34.00 ± 22.30 |
| | 28th | 54.24 ± 0.91 | 57.68 ± 3.14 | 51.62 ± 2.49 | 54.94 ± 3.21 | 57.28 ± 3.18 | 55.82 ± 4.22 | 53.58 ± 5.29 |
| CREA (μmol/L) | 7th | 22.00 ± 3.53 | 24.00 ± 4.18 | 20.60 ± 5.22 | 27.00 ± 6.16 | 28.20 ± 2.77 | 27.20 ± 4.15 | 24.20 ± 3.35 |
| | 14th | 22.80 ± 4.49 | 28.00 ± 2.00 | 27.60 ± 4.93 | 28.20 ± 5.81 | 30.60 ± 2.41 | 27.20 ± 3.03 | 37.00 ± 3.87 |
| | 28th | 20.40 ± 3.91 | 26.60 ± 2.30 | 24.20 ± 7.69 | 22.00 ± 3.54 | 27.20 ± 4.15 | 25.00 ± 3.61 | 27.80 ± 3.56 |
| URIC (μmol/L) | 7th | 279.80 ± 67.58 | 299.80 ± 106.21 | 249.00 ± 87.52 | 349.40 ± 160.63 | 410.40 ± 115.27 | 302.20 ± 50.19 | 318.00 ± 105.65 |
| | 14th | 243.80 ± 39.98 | 287.80 ± 73.41 | 259.80 ± 42.05 | 289.4 ± 82.99 | 319.80 ± 84.57 | 389.00 ± 86.20 | 393.00 ± 144.26 |
| | 28th | 206.60 ± 44.24 | 273.80 ± 52.18 | 321.40 ± 100.58 | 300.40 ± 40.07 | 262.20 ± 77.17 | 393.80 ± 136.11 | 450.40 ± 66.76 |

*The data were acquired at day 7, 14, and 28 after injection with rare-earth nanoparticles in mice. TBIL: Total bilirubin; AST: Aspartate aminotransferase; TP: Total proteins; URIC: Uric acid; CREA: Creatinine.

The results of the *in vivo* MRI characterization study demonstrated the distribution and circulation of the RENPs in the liver. The biochemical analysis of serum samples further indicated the physiological and pathological damage caused to mice organs and tissues, particularly liver and kidney, by RENPs. It is well known that liver and kidney are the main organs to metabolize endogenous or exogenous agents and serve as the sites for cholesterol synthesis and degradation.[21,22] The levels of some enzymes and substances such as ALT and CREA may directly reflect the functional statuses of these organs.[23] The biochemical analysis of serum revealed the adverse effects of RENPs on the liver and kidney of experimental mice, particularly those injected with 1.5 mg/kg $NaYbF_4$:Er nanoparticles.

The increase in the number of WBCs was indicative of inflammation in the mouse body that may probably cause fever or hematologic disease after particle injection.[23] Therefore, we suggest that the injected RENPs were mainly transported in the blood and metabolic organs such as the liver and kidney, which may explain how these particles induced injuries to the kidney and liver in our experiment.

Although our study has suggested that the use of RENPs may cause hepatotoxicity and nephritic toxicity in the animal, many strategies have been developed to minimize or avoid the risk of nanoparticles such as a surface coating of particles with silica, polymer, or proteins.[24-27] The direct interaction between nanoparticles (or rare-earth ions) and molecules in the cells may be mitigated through the use of these approaches. The rapid development of nanotechnology may facilitate progress in the field of nanomedicine and other biomedical applications. Considering the practical applications of nanomedicine, the results of the present study may provide a noteworthy explanation to understand the application of nanotechnology for future medical development.

In conclusion, our study has revealed the fact of obvious injuries to mouse liver and kidneys caused by the bare RENPs. The findings presented in this work may provide a fundamental understanding of the intrinsic toxicity associated with bare RENPs in animals. Moreover, our study would improve the understanding of the effects of long-term and high-dose treatment of RENPs on different organs.


## Financial support and sponsorship

This work was supported by grants from the Provincial Health and Family Planning Research of Fujian (No. 2016-1-43 and 2017-ZQN-32).


## Conflicts of interest

There are no conflicts of interest.

## References


1. Brockes JP, Kumar A. Appendage regeneration in adult vertebrates and implications for regenerative medicine. Science 2005;310:1919-23. doi: 10.1126/science.1115200.
2. Wu J, Xie L, Lin WZ, Chen Q. Biomimetic nanofibrous scaffolds for neural tissue engineering and drug development. Drug Discov Today 2017;22:1375-84. doi: 10.1016/j.drudis.2017.03.007.
3. Chen Q, Utech S, Chen D, Prodanovic R, Lin JM, Weitz DA, *et al.* Controlled assembly of heterotypic cells in a core-shell scaffold: Organ in a droplet. Lab Chip 2016;16:1346-9. doi: 10.1039/c6lc00231e.
4. Solanki A, Kim JD, Lee KB. Nanotechnology for regenerative medicine: Nanomaterials for stem cell imaging. Nanomedicine (Lond) 2008;3:567-78. doi: 10.2217/17435889.3.4.567.
5. Engel E, Michiardi A, Navarro M, Lacroix D, Planell JA. Nanotechnology in regenerative medicine: The materials side. Trends Biotechnol 2008;26:39-47. doi: 10.1016/j.tibtech.2007.10.005.

6. Viger ML, Grossman M, Fomina N, Almutairi A. Low power upconverted near-IR light for efficient polymeric nanoparticle degradation and cargo release. Adv Mater 2013;25:3733-8. doi: 10.1002/adma.201300902.
7. Li W, Wang J, Ren J, Qu X. Near-infrared upconversion controls photocaged cell adhesion. J Am Chem Soc 2014;136:2248-51. doi: 10.1021/ja412364m.
8. Chen Q, Xie X, Huang B, Liang L, Han S, Yi Z, *et al.* Confining excitation energy in Er3+ -sensitized upconversion nanocrystals through Tm3+ -mediated transient energy trapping. Angew Chem Int Ed Engl 2017;56:7605-9. doi: 10.1002/ange.201703012.
9. Teng X, Zhu Y, Wei W, Wang S, Huang J, Naccache R, *et al.* Lanthanide-doped Na(x)ScF(3+x) nanocrystals: Crystal structure evolution and multicolor tuning. J Am Chem Soc 2012;134:8340-3. doi: 10.1021/ja3016236.
10. Wu J, Chen Q, Liu W, He Z, Lin JM. Recent advances in microfluidic 3D cellular scaffolds for drug assays. Trends Analyt Chem 2017;87:19-31. doi: 10.1016/j.trac.2016.11.009.
11. Nel A, Xia T, Mädler L, Li N. Toxic potential of materials at the nanolevel. Science 2006;311:622-7. doi: 10.1126/science.1114397.
12. Cho WS, Cho M, Jeong J, Choi M, Cho HY, Han BS, *et al.* Acute toxicity and pharmacokinetics of 13 nm-sized PEG-coated gold nanoparticles. Toxicol Appl Pharmacol 2009;236:16-24. doi: 10.1016/j.taap.2008.12.023.
13. Arnaout CL, Gunsch CK. Impacts of silver nanoparticle coating on the nitrification potential of nitrosomonas europaea. Environ Sci Technol 2012;46:5387-95. doi: 10.1021/es204540z.
14. Wu J, Chen Q, Liu W, Lin JM. A simple and versatile microfluidic cell density gradient generator for quantum dot cytotoxicity assay. Lab Chip 2013;13:1948-54. doi: 10.1039/C3LC00041A.
15. Cai X, Lee A, Ji Z, Huang C, Chang CH, Wang X, *et al.* Reduction of pulmonary toxicity of metal oxide nanoparticles by phosphonate-based surface passivation. Part Fibre Toxicol 2017;14:13. doi: 10.1186/s12989-017-0193-5.
16. Tian J, Zeng X, Xie X, Han S, Liew OW, Chen YT, *et al.* Intracellular adenosine triphosphate deprivation through lanthanide-doped nanoparticles. J Am Chem Soc 2015;137:6550-8. doi: 10.1021/jacs.5b00981.
17. Vedunova MV, Mishchenko TA, Mitroshina EV, Ponomareva NV, Yudintsev AV, Generalova AN, *et al.* Cytotoxic effects of upconversion nanoparticles in primary hippocampal cultures. RSC Adv 2016;6:33656-65. doi: 10.1039/C6RA01272H.
18. Lin CH, Liu GF, Chen J, Chen Y, Lin RH, He HX, *et al.* Rare-earth nanoparticle-induced cytotoxicity on spatial cognition memory of mouse brain. Chin Med J 2017;130:2720-5. doi: 10.4103/0366-6999.218024.
19. Hou Y, Qiao R, Fang F, Wang X, Dong C, Liu K, *et al.* NaGdF4 nanoparticle-based molecular probes for magnetic resonance imaging of intraperitoneal tumor xenografts *in vivo*. ACS Nano 2013;7:330-8. doi: 10.1021/nn304837c.
20. Jang GH, Hwang MP, Kim SY, Jang HS, Lee KH. A systematic *in vivo* toxicity evaluation of nanophosphor particles via zebrafish models. Biomaterials 2014;35:440-9. doi: 10.1016/j.biomaterials.2013.09.054.
21. Fu AL, Shi XX, Zhang HJ, Fu B. Mitotherapy for fatty liver by intravenous administration of exogenous mitochondria in male mice. Front Pharmacol 2017;8:8. doi: 10.3389/fphar.2017.00241.
22. Futrakul N, Futrakul P. Biomarker for early renal microvascular and diabetic kidney diseases. Ren Fail 2017;39:505-11. doi: 10.1080/0886022X.2017.1323647.
23. Yonekawa O. An accurate diagnosis is possible with a systematic analysis of routine laboratory data. Rinsho Byori 2015;63:1072-9.
24. Sanvicens N, Marco MP. Multifunctional nanoparticles – Properties and prospects for their use in human medicine. Trends Biotechnol 2008;26:425-33. doi: 10.1016/j.tibtech.2008.04.005.
25. Albanese A, Tang PS, Chan WC. The effect of nanoparticle size, shape, and surface chemistry on biological systems. Annu Rev Biomed Eng 2012;14:1-6. doi: 10.1146/annurev-bioeng-071811-150124.
26. Ahamed M, Alsalhi MS, Siddiqui MK. Silver nanoparticle applications and human health. Clin Chim Acta 2010;411:1841-8. doi: 10.1016/j.cca.2010.08.016.
27. Soppimath KS, Aminabhavi TM, Kulkarni AR, Rudzinski WE. Biodegradable polymeric nanoparticles as drug delivery devices. J Control Release 2001;70:1-20. doi: 10.1016/S0168-3659(00)00339-4.

# 稀土纳米颗粒在小鼠中潜在的炎症和毒性风险的研究


## 摘要

**背景：**纳米技术是一种有望用于实现活体中的非侵入治疗与光学成像的工具。然而，近年来发展的纳米医学认为纳米颗粒在活体应用中有着潜在的毒性风险。在本研究中，我们以小鼠为模型，通过实验研究稀土纳米颗粒的潜在毒性。

**方法：**我们采用共沉淀法合成了稀土纳米颗粒。ICR小鼠随机分为七组，包括对照组和6组实验组（每组为10只小鼠），将该纳米颗粒注射入ICR小鼠，连续七天注射的浓度分别为0，0.5，1.0，和1.5毫克/千克。为进一步地评估这些稀土纳米颗粒在小鼠中的毒性，核磁共振成像被用于评估稀土纳米颗粒在小鼠中的吸收情况。同时，血液分析和生物分析用进一步地用于研究小鼠器官功能的受损程度。数据用平均值±标准差表示，并用单因素方差分析进行检验。重复测量分析用来评估每组中WBC（白细胞），ALT（谷丙转氨酶）和CREA（肌酐）随时间变化的差异性。

**结果：**我们成功地合成两种不同尺寸（10 nm 和 100 nm）的稀土纳米颗粒，并通过了投射电镜和980纳米激发激发条件下的光谱对合成的材料进行鉴定表征。更为重要的是，我们的核磁共振表征实验结果表明了该稀土纳米颗粒在小鼠肝脏中的分布和循环。另外，通过小鼠血常规检查发现实验组WBC明显增高，在28天时高至$(8.69\pm0.85) \times 10^9$/L（1.5 mg/kg $NaYbF_4$:Er处理组），表明稀土纳米颗粒可能引起小鼠体内的炎症反应。此外，生化分析结果显示1.5 mg/kg $NaYbF_4$:Er处理组ALT和CREA明显增高,在28天时分别达到$(64.20 \pm 15.50)$ U/L和$(27.80 \pm 3.56)$ μmol/L。通过这些结果我们发现稀土纳米颗粒可能对小鼠的器官和组织有着生理和病理方面的损伤，尤其是肝脏和肾脏。

**结论：**我们的研究预示着裸稀土纳米颗粒可引起潜在的动物肝毒性和肾毒性。